AIChE WILEY InterScience DISCOVER SOMETHING GREAT

FLUID MECHANICS AND TRANSPORT PHENOMENA

Drag Force of Intermediate Reynolds Number Flow Past Mono- and Bidisperse Arrays of Spheres

R. Beetstra, M. A. van der Hoef, and J. A. M. Kuipers
Faculty of Science & Technology, University of Twente, P.O. Box 217, 7500 AE Enschede, The Netherlands

DOI 10.1002/aic.11065
Published online January 2, 2007 in Wiley InterScience (www.interscience.wiley.com).

Extensive lattice-Boltzmann simulations were performed to obtain the drag force for random arrays of monodisperse and bidisperse spheres. For the monodisperse systems, 35 different combinations of the Reynolds number Re (up to Re = 1,000) and packing fraction ϕ were studied, whereas for the bidisperse systems we also varied the diameter ratio (from 1:1.5 to 1:4) and composition, which brings the total number of different systems that we considered to 150. For monodisperse systems, the data was found to be markedly different from the Ergun equation and consistent with a correlation, based on similar type of simulations up to Re = 120. For bidisperse systems, it was found that the correction of the monodisperse drag force for bidispersity, which was derived for the limit Re = 0, also applies for higher-Reynolds numbers. On the basis of the data, a new drag law is suggested for general polydisperse systems, which is on average within 10% of the simulation data for Reynolds numbers up to 1,000, and diameter ratios up to 1:4. © 2007 American Institute of Chemical Engineers *AIChE J,* 53: 489–501, 2007

Keywords: drag force, simulations, lattice Boltzmann, polydispersity

Introduction

From a purely theoretical point of view, surprisingly little is known about the force that a fluid, when flowing past an assembly of spheres, exerts on the individual particles. In fact, one could argue that the *only* exact result is the well-known Stokes-Einstein drag force $F_d = 3\pi\mu d u_o$ for a single, isolated sphere (dia. d), subject to Stokes flow (viscosity μ, flow velocity u_o). This result is valid in the limit where both the packing fraction ϕ, and the Reynolds number Re approach zero. The correction to the Stokes-Einstein drag due to the presence of neighboring particles has been evaluated in terms of an expansion in the packing fraction ϕ, but only the first few terms can be worked out analytically,[3] which limits its validity to packing fractions smaller than $\phi = 0.10$. For larger packing fractions, the drag force has to be estimated from approximate theoretical methods, such as those leading to the Brinkman equation, or from empirical data via Carman-Kozeny type relations.[4] There is a similar situation when the deviation from Stokes flow—now again for an isolated particle—is considered. The first-order correction to the Stokes-Einstein drag force for $\mathrm{Re} > 0$ was obtained analytically by Oseen in 1910, and terms up to order Re^5 were derived by Goldstein.[5] Unfortunately, already for Reynolds numbers as small as three, these expressions deviate markedly from the experimental data, and the conclusion is that for $\mathrm{Re} > 1$ these analytical solutions have little value.[6] Given the fact that the evaluation of the drag force for the two limiting cases $\phi \to 0$ and $\mathrm{Re} \to 0$ is already difficult, it will be clear that our understanding of fluid-solid interactions from a purely theoretical basis is very limited for systems in which *both* the packing fraction and Reynolds number are non-zero. Kaneda[7] was the first to derive an expression for the drag force in such systems, where he found that in the limit of $\mathrm{Re} << \sqrt{\phi} << 1$ the first inertial contribution to the drag-force scales as Re^2. Later theoretical work[8,9] has confirmed the Re^2 scaling for the first inertial contribution, at least for

Correspondence concerning this article should be addressed to M. A. van der Hoef at M.A.vanderhoef@utwente.nl.

ordered arrays, and was found consistent with data from numerical simulations. Nevertheless, the practical value of these theories is rather limited since they are restricted to very low-Reynolds numbers and small packing fractions. For this reason, historically one has resorted to empirical data for either the pressure drop (for packed beds) or terminal velocities of sedimenting particles (and bed expansion experiments), to obtain estimates for the gas-solid drag for $\mathrm{Re} > 1$ and $\phi > 0.1$. One of the problems is that such data only provides indirect information on the drag force, for systems which are very different, and often not well-defined in terms of homogeneity, monodispersity, sphericity of the particles, mobility, and so on. This has resulted in a large number of empirical relations for the gas-solid drag force,[10] and although the relations by Ergun[1] and Wen and Yu[11] are the most widely used, there is at present no real consensus as to what the most accurate prediction for the drag force is at a given Reynolds numbers and packing fraction. Thus far, all correlations were based on experimental data, however, very recently a new correlation has been proposed on the basis of lattice-Boltzmann simulation data.[2] One of the biggest advantages of simulations is that the material and/or flow conditions can be perfectly controlled, which is often not the case in experiments. For instance, the Ergun correlation is widely used for beds of perfectly monodisperse, spherical particles, whereas Ergun derived his equation from data which not only involved spheres, but also sand and pulverized coke.[1] With the advancement of computer resources, direct numerical simulations methods (such as the lattice-Boltzmann method) have become a viable alternative for acquiring accurate data on the gas-solid drag force, from which new "empirical" correlations can be derived for well-defined systems.

In this article, we want to present the results of extensive lattice-Boltzmann (LB) simulations of both monodisperse and bidisperse systems, for packing fractions ranging from $\phi = 0.10$ to $\phi = 0.65$, and Reynolds numbers in the range of 10–1,000, where results for the limit $\mathrm{Re} \to 0$ have been published in a previous article,[12] to which we refer, hereafter, as reference I. The data which we present here for bidisperse systems are to our knowledge the first of this kind. For monodisperse systems, however, as mentioned earlier, similar type of simulations have been performed previously.[2] The justification for also including monodisperse results in this article is that we extended the Reynolds number range up to 1,000, where the data of Hill et al.[2] was limited to $\mathrm{Re} < 120$. More generally, the focus of the Hill et al.[2] article was to contribute to the fundamental understanding of inertial flow in particulate systems, and not so much aimed at providing a drag force relation for practical use. For instance, they do not provide a correlation over the entire range $0 < \mathrm{Re} < 120$, but only for small Re (typically < 2), and for $\mathrm{Re} > 40$. Moreover, for the latter range they suggest a functional form $F = F_2(\phi) + F_3(\phi)\ \mathrm{Re}$ where only for $F_3(\phi)$ the explicit functional form is given. The validity of this expression for $\mathrm{Re} > 120$ is not clear either. In the limit $\phi \to 0$ and $\mathrm{Re} \to \infty$, the Hill-Koch-Ladd expression corresponds to a drag coefficient $C_d = 1.09$, which is more than a factor of two larger than the commonly accepted range of 0.40–0.44.

The purpose of this article is to provide a new drag force correlation for mono- and polydisperse systems for a large range of Reynolds numbers and packing fractions, based on lattice Boltzmann data. The main motivation for constructing such a correlation is that effective fluid-solid drag laws are a key input in the numerical models for dense particle-laden flows (for example, gas-fluidized beds), and are, therefore, of crucial importance in chemical engineering.[13] For this reason, the functional form of our final correlation is determined completely by the requirements of accuracy and simplicity, and not by theoretical considerations. For instance, we will not make use of the fact that the drag force scales as Re^2 for very small Reynolds numbers, since this would make the functional form much more complicated without providing a better fit to the data in the Reynolds number range that is relevant for industrial applications. In a previous article[13] we have reported on a preliminary fit to part of our data, to serve as an illustration of the multiscale modeling approach. In this work, we present a more extensive and more precise fit.

In the next two sections we will first give an overview of the drag force relations for monodisperse and bidisperse systems. This is followed by a short recapitulation of the simulation procedure, the details of which can be found in reference 1.

Overview of Drag Force Relations for Monodisperse Systems

Before presenting the various drag force relations that have appeared in literature, it is essential to first carefully define the various quantities of interest, in particular since there exists some ambiguity in literature in the way the Reynolds number and the drag force are defined. To this end, we consider a static bed of N monodisperse spheres (dia. d, volume V_p), at a packing fraction $\phi = NV_p/V$, where V is the total volume of the system. When a gas (or a liquid) flows through the bed with a constant velocity $\mathbf{u}_o$, a particle experiences two forces from the fluid, namely the drag force $\mathbf{F}_d$ due to the fluid-solid friction at the surface of the spheres, and a force $\mathbf{F}_b = -V_p \nabla P$ due to the static pressure gradient ∇P, which drives the gas flow. The sum of $\mathbf{F}_d$ and $\mathbf{F}_b$ is the total force $\mathbf{F}_{g\to s}$ that the gas phase exerts on a solid particle, which is sometimes also referred to as the drag force. From a balance of forces follows that $V\nabla P = N\mathbf{F}_{g\to s}$; eliminating ∇P from the expressions gives that $\mathbf{F}_d = (1-\phi)\mathbf{F}_{g\to s}$, and, thus, the two definitions for the drag force differ by a factor of $1-\phi$. In this paper, we define $\mathbf{F}_d$ as the drag force, which is the common choice in chemical engineering.[10] Since there exists an exact expression for the drag force on an isolated particle in the limit of zero Reynolds number—the aforementioned Stokes-Einstein relation $3\pi\mu d\mathbf{u}_o$—it is natural to use this expression to normalize the drag force at arbitrary packing fractions and flow velocities. We, thus, define the dimensionless drag force F as

$$F(\phi, \mathrm{Re}) = \mathbf{F}_d / 3\pi\mu d\mathbf{U}, \quad \text{so that} \quad F(0,0) = 1 \qquad (1)$$

Note that in this definition we have used the superficial velocity $\mathbf{U} = (1-\phi)\ \mathbf{u}_o$ instead of average fluid-flow velocity $\mathbf{u}_o$. As is indicated in Eq. 1, the dimensionless drag

force F will only depend on other dimensionless parameters which characterize the system, which are the packing fraction ϕ and the particle-Reynolds number Re, defined by

$$\mathrm{Re} = \frac{\rho_g U d}{\mu} = \frac{\rho_g (1-\phi) u_o d}{\mu} \tag{2}$$

with ρ_g the density of the gas phase. In chemical engineering literature, the gas-particle interaction is often represented in terms of a pressure drop per unit length $\bigtriangledown P$ rather then a drag force. The relation between $\bigtriangledown P$, and the dimensionless drag force defined by (Eq. 1) is

$$F = -\left(\frac{1-\phi}{\phi}\right)\frac{\nabla P d^2}{18\mu U}$$

Basically two classes of relations can be found in literature to describe the drag force for general flow conditions. The first class of relations is based on the expression for the drag force in the limit of Stokes flow $F(\phi, 0)$, to which a term linear in Re is added to account for inertial effects, viz

$$F(\phi, \mathrm{Re}) = F(\phi, 0) + \alpha(\phi)\mathrm{Re} \tag{3}$$

The second class of relations is based on the expression for the drag force on a single particle $F(0, \mathrm{Re})$, where the influence of the neighbouring particles is accounted for by multiplying with a power of the voidage, viz

$$F(\phi, \mathrm{Re}) = F(0, \mathrm{Re})(1-\phi)^{-\beta} \tag{4}$$

where β is usually taken as a constant, independent of Re.

We start with the first representation, which has the longest history. In the 1920s, Blake,[14] Kozeny,[15] and Burke and Plummer[16] suggested the following expressions for the functional form of $F(\phi, 0)$ and $\alpha(\phi)$

$$F(\phi, 0) = \frac{a\phi}{18\,(1-\phi)^2}, \quad \alpha(\phi) = \frac{b}{18\,(1-\phi)^2} \tag{5}$$

Ergun[1] obtained the values $a = 150$ and $b = 1.75$ on the basis of data for the pressure drop over packed beds of various materials (sand, spheres, pulverized coke) from 640 different experiments; the combination of Eqs. 3 and 5 with these values for a and b has become known as the Ergun correlation, and is one of the most widely used expressions for fluid-solid drag, even to date. More recent experiments showed that three main regimes exist in fluid flow through packed beds, where for each regime a different set of parameters a, b was derived.[17] In particular, for $\mathrm{Re} < 2.3$: $a = 192$, b = 0: for $5 < \mathrm{Re} < 80$: $a = 182$, $b = 1.92$; and for $\mathrm{Re} > 120$: $a = 225$, $b = 1.61$. Since 1999 also accurate numerical-simulation data for the drag force has become available from three different research groups,[9,12,18] using the lattice-Boltzmann method. For dense beds at low-Reynolds numbers, all three research groups concluded that expression (Eq. 5) for $F(\phi, 0)$ provides an accurate representation of the drag force if a coefficient $a = 180$ is used, which corresponds to the Carman[19] equation. One of the shortcomings of expression (Eq. 5), however, is that its validity is limited to dense beds. In reference 1 it was shown that the following simple modification of the Carman equation provides the best fit to all simulation data for arbitrary packing fractions

$$F(\phi, 0) = \frac{180\phi}{18(1-\phi)^2} + (1-\phi)^2(1 + 1.5\sqrt{\phi}) \tag{6}$$

The lattice-Boltzmann simulations have been extended also to intermediate Reynolds number flow.[2,20] On the basis of their data in the range $40 < \mathrm{Re} < 120$, Koch, Hill and Ladd[2] suggest an expression for the form-drag coefficient $\alpha(\phi)$ which is different from the Burke and Plummer expression (Eq. 5)

$$\alpha(\phi) = 0.03365\,(1-\phi) + 0.106\,\phi(1-\phi) + \frac{0.0116}{(1-\phi)^4} + \frac{\delta F}{\mathrm{Re}} \tag{7}$$

where we have added a term δF/Re which is not found in Hill et al.,[2] and needs some clarification. In their article, Hill et al., define two expressions for the normalized drag force:[†] $F = F_0(\phi) + F_1(\phi)\ \mathrm{Re}^2$ for very small Re (typically smaller than 2), and $F = F_2(\phi) + F_3(\phi)$ Re for $\mathrm{Re} > 40$. If $F_0(\phi) = F_2\ (\phi)$ then $\alpha(\phi)$ as defined by (3) would be equal to $F_3(\phi)$, since $F(\phi, 0) = F_0(\phi)$. However from table 1 of Hill et al.[2] it can be seen that there are some small differences between the numbers for F_2 and F_0. Unfortunately, Hill et al. have only provided a fit for F_0, and not for F_2, and for this reason researchers have neglected the difference when applying the Hill-Koch-Ladd correlation, which is justified for $\mathrm{Re} > 200$, but not for smaller Reynolds numbers. The data from Hill-Koch-Ladd shows that the difference $\delta F = F_2 - F_0$ as a function of ϕ is rather scattered, which makes it difficult to identify a clear trend. On the basis of their data, we have made the following rough estimate for δF

$$\delta F = \frac{6\phi - 10\phi^2}{(1-\phi)^2} \tag{8}$$

where again we stress that the actual data is strongly fluctuating around this fit, particularly for $\phi < 0.2$. Nevertheless, the use of this δF in expression (7) will give a better estimate of the Hill- Koch-Ladd data for Reynolds numbers smaller than 200, compared to setting $\delta F = 0$. The lattice Boltzmann simulations of Kandhai et al.,[20] performed in the range $\mathrm{Re} < 70$, were found to be consistent with the results by Hill et al.

The second class of drag force relations (4) is based on the expression for the normalized drag force on a single particle $F(0, \mathrm{Re})$, which is traditionally described in literature by a drag coefficient $C_d = 24F(0, \mathrm{Re})/\mathrm{Re}$. Finding accurate estimates for $F(0, \mathrm{Re})$ has challenged the scientific community for a large number of years. As mentioned in the introduction, an evaluation from theory proves to be a cumbersome route, so that our current knowledge of $F(0, \mathrm{Re})$ is mainly based on experimental data, from which one can roughly distinguish four different flow regimes. For $\mathrm{Re} << 1$ there is the Stokes flow regime, for which by definition $F(0, \mathrm{Re}) = 1$. For $\mathrm{Re} > \mathrm{O}(10^3)$ the drag force is found to scale linearly with the Reynolds number: $F(0, \mathrm{Re}) = c\ \mathrm{Re}/24$

[†]Note that the definitions of the drag force, and the Re number are different in the Hill et al. article.

Table 1. Some Well-Known Empirical Correlations for the Normalized Drag Force on an Isolated Particle

Schiller & Nauman (1935):[23]	$F(0,\mathrm{Re}) = \begin{cases} 1 + 0.15\ \mathrm{Re}^{0.687} & (\mathrm{Re} < 10^3) \\ \frac{0.44}{24}\mathrm{Re} & (\mathrm{Re} > 10^3) \end{cases}$
Dallavalle (1948):[38]	$F(0,\mathrm{Re}) = 1 + 0.2624\ \mathrm{Re}^{0.5} + \frac{0.413}{24}\mathrm{Re}$
White (1974):[37]	$F(0,\mathrm{Re}) = 1 + \frac{0.25\ \mathrm{Re}^{0.5}}{1+\mathrm{Re}^{-0.5}} + \frac{0.4}{24}\mathrm{Re}$
Turton & Levenspiel (1986):[39]	$F(0,\mathrm{Re}) = 1 + 0.173\ \mathrm{Re}^{0.657} + \frac{0.413}{24}\left(\frac{\mathrm{Re}}{1+16300\mathrm{Re}^{-1.09}}\right)$

Note that the traditional representation for the drag force in this limit is via a drag coefficient $C_d = 24F(0, \mathrm{Re})/\mathrm{Re}$.

with c in the range 0.40–0.44, which is referred to as the Newton flow regime. The regime $1 < \mathrm{Re} < \mathrm{O}(10^3)$ can be viewed as a transition regime from Stokes flow to Newton flow (sometimes referred to as Allen flow), for which the functional form of the drag force is not *a priori* obvious. And finally, for large-Reynolds numbers ($\mathrm{Re} > 10^5$), a sudden drop in the drag force occurs (the critical transition), after which it again seems to grow linear with Re. A large number of empirical relations for the subcritical region $\mathrm{Re} < 10^5$ have been suggested over the years, a selection of which are listed in Table 1, and also shown in Figure 1, together with the experimental data.[21]

The modification of the single-particle-drag force to account for the presence of neighboring particles has been determined experimentally by fitting the ratio $v_t(0)/v_t(\phi)$ to a function $(1 - \phi)^{-n}$, where $v_t(\phi)$ and $v_t(0)$ are the terminal velocities of an assembly of spheres and an isolated sphere, respectively. Apart from sedimentation experiments, also fluidization experiments have been used to estimate the value n. On the basis of the experimental data, various expressions for n as a function of the Reynolds number have been suggested; an overview is given by Di Felice.[10] Unfortunately, it is not possible to derive a general relation between β in Eq. 4 and n, since this depends on how the nondimensionless drag force F_d scales with v_t. For very low-Reynolds numbers $F_d \sim v_t$ which gives $\beta = n - 1$, while for higher-Reynolds number, one may assume that $F_d \sim {v_t}^2$ which yields $\beta = 2n - 1$. Richardson et al.[22] found that $n = 4.65$ for $\mathrm{Re} < 0.2$, and $n = 2.4$ for $\mathrm{Re} > 500$, which values thus correspond to $\beta = 3.65$, and $\beta = 3.8$, respectively. For this reason, Wen and Yu[11] suggested a drag force relation of the type (Eq. 4) with a constant value $\beta = 3.7$ for the entire Reynolds-number range, in combination with the Schiller and Nauman[23] expression for $F(0, \mathrm{Re})$, which was at that time regarded as the most accurate relation. The Wen and Yu correlation has remained very popular in chemical engineering ever since. Di Felice[24] found that the power β is weakly dependent on the Reynolds number, and proposed the following modification to the value 3.7:

$$\beta = 3.7 - 0.65 \exp\left\{\frac{-(1.5 - \log \mathrm{Re})^2}{2}\right\} \tag{9}$$

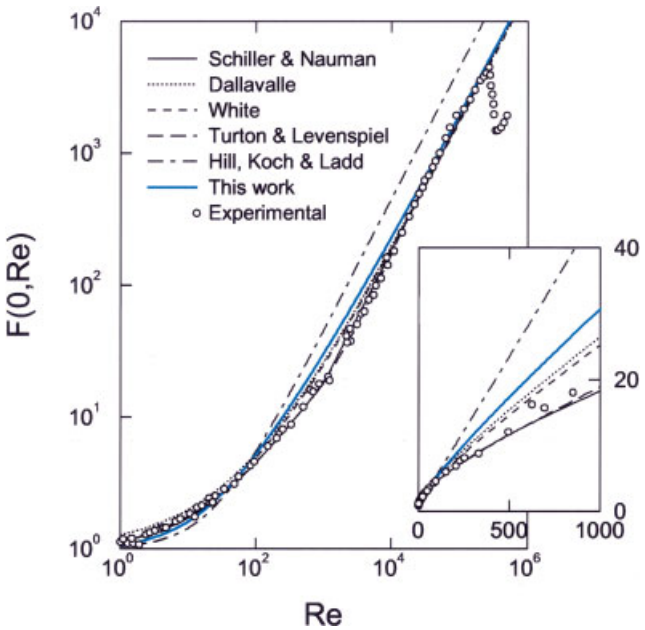

Figure 1. Normalized drag force for an isolated particle as a function of the Reynolds numbers, on a log-log scale.

Shown are the various empirical correlations from table 1, together with the $\phi = 0$ limit of the correlation from Hill et al.,[2] and from this article (see simulation results for monodisperse systems section). The range below Re = 1,000 is shown on a linear scale in the inset. The experimental data are taken from the book of Schlichting[21]. [Color figure can be viewed in the online issue, which is available at www.interscience.wiley.com.]

This approach is particularly popular in sedimentation literature and liquid fluidization.

Both type of correlations (3) and (4) have their relative merits and weaknesses, which makes them to some extend complementary. The "Ergun type" relations (3) are only valid for denser systems, whereas the "Wen and Yu" type relations have been derived on the basis of data from relatively dilute systems. For this reason, Gidaspow has suggested to use the Ergun equation for packing fractions higher than $\phi = 0.2$, and the Wen and Yu equation for lower-packing fractions.[25] The disadvantage of such a drag law is that there is a discontinuity at $\phi = 0.2$, and also it is questionable whether the Ergun equation can be extrapolated to such high-porosities. Nevertheless, this hybrid Ergun-Wen and Yu drag law is widely used in chemical engineering, and for this reason we will compare it with our lattice Boltzmann results later in this work. A different approach to combining expressions of the type (3) and (4) has been followed by Gibilaro et al.[26] They suggest a function

$$F(\phi, \mathrm{Re}) = f(\mathrm{Re})(1-\phi)^{-3.8}, \quad f(\mathrm{Re}) = \frac{17.3}{18} + \frac{0.336}{18}\mathrm{Re} \tag{10}$$

where f(Re) is chosen such that $F(\phi, \mathrm{Re})$ is equal to the Ergun equation for $\phi = 0.6$. Note that in the limit $\phi \to 0$, $\mathrm{Re} \to 0$ expression (Eq. 10) leads to $F = 0.96$, thus, very close the Stokes-Einstein result; taking the limit $\phi \to 0$, $\mathrm{Re} \to \infty$ shows that Eq. 10 leads to a drag coefficient $C_d = 0.448$, which is very close to the experimental value. There is no doubt that expression (Eq. 10) represents a very useful unification of the Ergun, Wen and Yu type expressions, and is also backed by experimental data.[26] However one may argue if the "true" drag force would indeed take such a simple form as given by Eq. 10, or more generally by equations of the type (3) and (4). In particular, the dependence on the packing fraction $\sim (1-\phi)^{-\beta}$ of (3) seems oversimplified, when compared to the most accurate expression (6) for the limit $\mathrm{Re} \to 0$. Also, the linear scaling with the Reynolds number of Eq. 3 seems to be an oversimplified representation for the sub-Newton-flow regime ($\mathrm{Re} < 1{,}000$).

In this work we want to come to a single correlation where the scaling with both the Reynolds number and the packing fraction is re-evaluated. This expression will be based on the data of lattice Boltzmann simulations for 35 different combinations of ϕ, and Re in the range $\phi = 0.4 - 0.9$ and $\mathrm{Re} = 20 - 1{,}000$. For the limit $\mathrm{Re} = 0$ the correlation should satisfy expression (Eq. 6), whereas in the limit $\phi = 0$ we will constrain our correlation to approach the widely accepted value $F(0, \mathrm{Re}) = 0.413\ \mathrm{Re}/24$ in the limit $\mathrm{Re} \to \infty$. We will discuss this in detail in the simulation results for monodisperse systems section.

Drag Force for Polydisperse Systems

For a random array of polydisperse particles, two additional parameters for each species are required to characterize the system, for instance the diameter d_i, and the number of particles N_i of species i. It is more convenient, however, to characterize the system by the dimensionless parameters x_i and y_i which carry the same information

$$x_i = \frac{\phi_i}{\phi}, \quad y_i = \frac{d_i}{\langle d \rangle}$$

where $\phi_i = N_i \pi d_i^3/6V$ is the individual packing fraction of species i, and $\langle d \rangle$ is the Sauter mean diameter, which is defined as

$$\langle d \rangle = \frac{\sum_{i=1}^{c} N_i d_i^3}{\sum_{i=1}^{c} N_i d_i^2} = \left[\sum_{i=1}^{c} \frac{x_i}{d_i} \right]^{-1} \tag{11}$$

where c is the number of species present in the system. If $\mathbf{F}_{d,i}$ is the individual drag force on a sphere of species i, then we define the individual normalized drag force F_i as

$$F_i = \mathbf{F}_{d,i}/3\pi\mu d_i \mathbf{U} \tag{12}$$

In principle, the normalized drag force will depend on all the dimensionless parameters which characterize the systems, that is $F_i(\phi, \mathrm{Re}; x_1, x_2, \ldots, x_c; y_1, y_2, \ldots, y_c)$.

In literature, the gas-solid interaction in polydisperse systems is mainly studied in terms of the sedimentation velocities of the individual species, which can be obtained directly from experiments. For dilute arrays in the limit of zero-Reynolds number, Batchelor[27] derived an explicit expression for the sedimentation velocities, which corresponds to a normalized drag force

$$F_i = \frac{1-\phi}{1 + \sum_{j=1}^{c} S_{ij}\phi_j}$$

The diagonal terms S_{ii} take the same value -6.55 as was derived for monodisperse systems. The other coefficients depend on the diameter and density ratios, and are not symmetrical (that is, $S_{ij} \neq S_{ji}$).[28] For higher-volume fractions and Reynolds number, one has to resort to empirical data for the sedimentation velocities to determine the gas-particle interaction forces. On the basis of this data (mainly for bidisperse systems), various corrections to the monodisperse drag force have been proposed, in order to account for polydispersity (for example, see Di Felice,[10] and references therein). The problem with these kind of experiments is the particles segregate while falling, so that locally the mass fraction of the species—and, thus, also $\langle d \rangle$—is not constant. Also, the experiments only give indirect information on the drag force. Although several methods have been developed to measure the drag force on a particle directly,[29,30,31] these are all limited to single particles or particles that are surrounded by only a few others, which cannot be representative of a bi- or polydisperse system.

The approach that is most often encountered in numerical modeling of large scale gas-binary solid flow is to assume that a particle experiences the same normalised drag force as it would in a monodisperse system of equal overall porosity, with the Reynolds number Re replaced by the individual value $\mathrm{Re}_i = \rho_g U d_i/\mu$ (for example, see Gidaspow[25]). Patwardhan and Tien[32] suggested a more refined model, in which a different effective packing fraction for each species is used, instead of the same overall packing fraction. They

assumed that the porosity that a particle experiences is mainly determined by the ratio of the average-pore size to its diameter. This means that in a binary mixture the smaller (larger) particles will experience a larger (smaller) porosity, since the pores are large (small) compared to their diameter. In our previous study on binary systems at low-Reynolds numbers, we found that using the same overall packing fraction (that is, the approximation $F_i = F(\phi)$) gave a drag force that was almost a factor of five different from the simulation results, for a dia. ratio 1:4. A much better agreement with the simulation data was obtained when using an effective porosity as suggested by Patwardhan and Tien.[32] Also excellent agreement was found with the new expression

$$F_i = ((1-\phi)\, y_i + \phi\, y_i^2 + 0.064(1-\phi) y_i^3)\, F(\phi, 0) \qquad (13)$$

which we derived on the basis of the Carman-Kozeny approximation. The advantage of Eq. 13 over the Patwardhan and Tien model is that it is much simpler to evaluate. In this work, we will test if the same modification (Eq. 13) can be applied to the bidisperse drag force at higher-Reynolds numbers.

Very recently, Okayama et al.[33] studied segregation in a bidisperse-fluidized beds by numerical simulation in which they used 4 different models for the individual drag force on the particles. They subsequently compared with experiments of the same system in order to validate the various models. Specifically, they used a model *A* where the dia. d in the expression for the actual (that is, non-normalized) drag force for a monodisperse system, is replaced by the individual diameter of the particles, which is the equivalent to setting $F_i = F(\phi, \mathrm{Re}_i)$. In the other three models B1–B3, they replace the dia. d in the expression of the non-normalized drag force for a monodisperse system by the Sauter-mean diameter, and, subsequently, distribute this force to the individual particles by ratio of the particle diameter (B1), projected surface (B2), and volume (B3). In our notation, the model *BN* corresponds to $F_i = y_i^{N-1}\, F(\phi, \langle \mathrm{Re} \rangle)$, with $N = 1$, 2, 3. The data from Okayama et al. indicates that the experimental segregation rate lies in between the predictions that are made by the simulations using drag model B2 and B3, respectively, which seems to indicate that the true individual drag force should be decribed by a combination of model B2 and B3, as is indeed the case in our expression (Eq. 13).

Simulation Method

The simulation procedure that we use to determine the drag force has been discussed in detail in reference I. We will quickly reiterate the most important aspects. In the simulations we make use of the lattice-Boltzmann (LB) method to resolve the flow of gas around the particles, where stick boundary conditions are employed at the surface of the particles. In the LB method, space and time are discretized, and the information on the local gas momentum and density is contained in the single gas-particle distribution function, which is updated via a discretized version of the Boltzmann equation.[34] The change in gas momentum per unit time, required to maintain stick boundary conditions at the surface of a solid particle i, is equal to the total force $-\mathbf{F}_{g\to s,i}$ that the particle i exerts on the gas phase, from which the drag force can be obtained.[35] Due to the discretization of the surface, the precise diameter of a spherical particle is not well-defined. Therefore, a calibration run needs to be performed for each individual boundary configuration, where the measured drag force for a dilute cubic array for low-Reynolds numbers is compared with the exact expression by Hasimoto,[36] from which the effective diameter can be obtained. The same effective diameter is used for the simulations at finite Reynolds numbers. Note that in the LB model, all quantities are in units of the time step δt, and the lattice spacing δl, but a conversion to SI units is not required since in the end we are only interested in the relation between the dimensionless quantities F, Re and ϕ.

For the monodisperse simulations, $N = 54$ particles with an effective dia. d are distributed randomly in a box of $n_x \times n_y \times n_z$ lattice sites via a Monte Carlo procedure, where d has a value typically in between 17 and 26 lattice spacings. For these values the size of the box can always be chosen such that packing fraction $\phi^{\mathrm{sim}} = N\pi d^3/(6 n_x n_y n_z)$ is within 1% of the desired packing fraction ϕ. The result for the drag force is then extrapolated to exactly ϕ by a second order Taylor expansion using an initial estimate for the drag force as a function of ϕ. Periodic boundary conditions are used. All spheres are forced to move with the same constant velocity $\mathbf{v}^{\mathrm{sim}}$ in some arbitrary direction, so that the array of spheres moves as a static configuration through the system. A uniform force is applied to the gas phase, to balance the total force $-\sum_{i=1}^{N} \mathbf{F}_{g\to s,i}$ from the moving particles on the gas phase. From this follows that in a frame of reference where the particles are static, the superficial flow velocity U is equal to $-\mathbf{v}^{\mathrm{sim}}$, so that $\mathrm{Re} = \rho d |\mathbf{v}^{\mathrm{sim}}|/\mu$, where the density $\rho = 36$ in LB units. Once an equilibrium state is obtained, the average value $\overline{\mathbf{F}}_{g\to s} = \langle \sum_{i=1}^{N} \mathbf{F}_{g\to s,i}/N \rangle_t$ is determined, with $\langle \cdot \rangle_t$ a time average. A second average $\langle \cdot \rangle_c$ is performed over typically 10–30 different-particle configurations and flow directions, so that the final estimate for the dimensionless drag force from the simulations is $F(\phi, \mathrm{Re}) = -(1-\phi)\langle \overline{\mathbf{F}}_{g\to s} \rangle_c / 3\pi\mu d \mathbf{v}^{\mathrm{sim}}$, where the error in the data is determined from the standard deviation σ of F in the average $\langle \cdot \rangle_c$. Note that there can be large fluctuations in the outcome of the different configurations, and for this reason we did not include any data which deviated more than 2.5 σ from the mean value. Note that simulation procedure of Hill, Koch and Ladd is slightly different, where the particles are held static and a gas flow is induced by applying a uniform body force.[9] One of the advantages of our procedure is that the Reynolds number is *set*, whereas in Hill, Koch and Ladd the Reynolds number has to be measured, which introduces additional uncertainties. The error in our data for the drag force is on average 2.5%, which is comparable to the error margins reported by Hill, Koch and Ladd.

The actual quantity of interest, however, is not F itself, but rather the *deviation* of the drag force from the low-Reynolds number limit $F(\phi, 0)$, since for the latter we already have an accurate representation (6). Hence, from the simulation data we evaluate the quantity α as defined in Eq. 3, but now in a generalized form so that it can also be dependent on the Reynolds number

$$\alpha(\phi, \mathrm{Re}) = (F(\phi, \mathrm{Re}) - F(\phi, 0))/\mathrm{Re} \qquad (14)$$

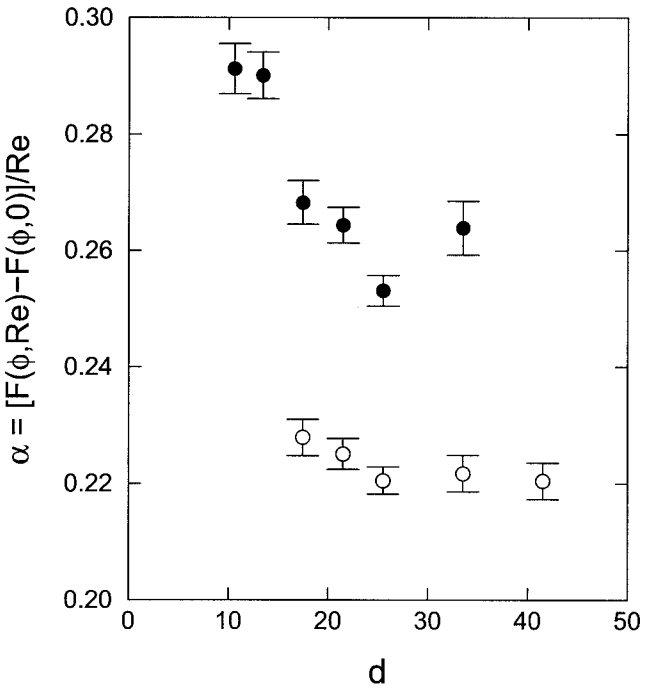

Figure 2. Simulation data for the drag force at finite Re minus the simulation data at Re = 0, divided by Re, as a function of the particle diameter.

The filled circles are for Re = 210, the open circles for Re = 1049. The diameter is in units of lattice spacings of the lattice Boltzmann model. The packing fraction is equal to $\phi = 0.5$. Note that for this packing fraction Eq. 7 gives $\alpha = 0.2375 + 1.85/\mathrm{Re}$, whereas the Ergun relation[1] predicts $\alpha = 0.389$, independent of the Reynolds number.

For evaluating α from simulation, we use for $F(\phi, 0)$ the raw simulation data as shown in Figure 2 and 3 of reference I, and *not* expression (6), which represents the extrapolated, grid-independent result for $F(\phi, 0)$. The reason is that this way any of the Re = 0 finite size effects and fluctuations in $F(\phi, \mathrm{Re})$ are automatically canceled, since the Re > 0 simulations are performed for exactly the same configurations, diameters and shear viscosity $\mu = 0.03$ (in LB units) as in the simulation reported in reference I. An important issue which remains to be addressed is whether the resolution of the grid that we use is sufficiently high to yield reliable results, in particular for higher-Reynolds numbers. In our simulations, we reach Reynolds numbers of up to 1,000, which is clearly far beyond the laminar regime, and even may be in the turbulent regime—depending on how 'turbulence' is precisely defined. The lattice-Boltzmann model is in principle well capable of modeling turbulent flow, provided that the grid resolution is high enough so that all the relevant length-scales are captured.[34] In this respect there exists no difference with direct numerical simulations utilizing finite-difference or finite-volume techniques. It is difficult to precisely pinpoint what resolution is "sufficient" for these type of simulations, which also depends on the packing fraction of the spheres. Also it is not clear if a lack of resolution will affect the *average* gas-solid momentum exchange in the same way as it would affect for instance the *instanteneous* fluid-flow profiles. In order to test the effect of the grid resolution on the drag force, we have evaluated α for various values of the dia. d, keeping the Reynolds number Re constant. In Figure 2 we show the simulation result for α as a function of the particle diameter in lattice-Boltzmann units, for a typical packing fraction $\phi = 0.5$. We find that for the highest-Reynolds number (Re = 1049) the data is independent of the particle size for diameters larger than 25 lattice units. For the lower Reynolds number (Re = 210) the fluctuations are larger, but also no clear trend can be observed beyond diameters of 17 lattice units. We did an additional test for an even denser system ($\phi = 0.6$) at the largest Reynolds number (Re = 1049), which is the most difficult case for the simulation to resolve, since the space between the particles is the smallest. We found that the difference in α using a diameter of 25 and 34 lattice spacings was only 2.2%, which is comparable to the error in the simulation data itself. On the basis of the observations from Figure 2, we have performed all simulations at packing fractions above $\phi = 0.3$ for two diameters: $d = 17.5$ and $d = 25.5$, where the final estimate for $\alpha(\phi, \mathrm{Re})$ is then obtained as the average of the two results. For packing fractions 0.3, 0.2 and 0.1 we have used the $d = 17.5$ data only.

The procedure for binary systems is essentially the same as for the monodisperse systems, only that we now collect the data for the drag force on type 1 and type 2 particles sep-

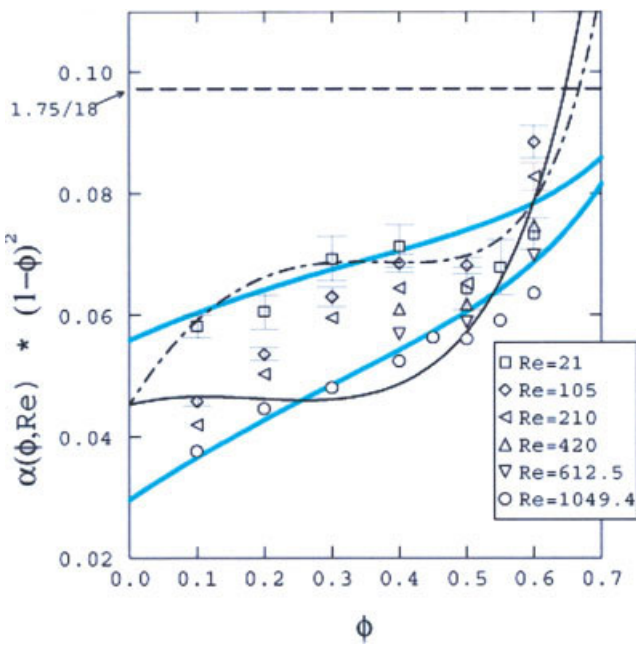

Figure 3. α multiplied by the porosity squared, as a function of the packing fraction.

The symbols are the simulation data from this work for various Reynolds numbers (see legend). The error bars are only shown when larger than the size of the symbols. The black dashed line is the Ergun equation $\alpha (1 - \phi)^2 = 1.75/18$; The black solid line represents expression (7) by Hill et al.,[2] with $\delta F = 0$. The dot-dashed line is expression (7) with δF given by (8), for Re = 40. The lower and upper grey line is the prediction from our best fit Eq. 16 at Re = 1049.4, and Re = 21, respectively. [Color figure can be viewed in the online issue, which is available at www.interscience.wiley.com.]

arately, that is, we calculate the individual drag force as $F_1 = -(1-\phi)\ \langle\langle\sum_{i=1}^{N1}\ \mathbf{F}_{g\to s,i}/N_1\rangle_t\rangle_c/3\pi\mu d_1\mathbf{v}^{\mathrm{sim}}$, where the summation Σ_i is over type 1 particles only. Another difference with the monodisperse simulations is that the diameters are on average somewhat smaller (due to the larger number of particles) so that the finite size effects are more apparent. Test runs for different diameters showed that the simulation data for α_i was scaling roughly as $1/\langle d\rangle^2$, so that in all cases simulations for two values of $\langle d\rangle$ have been performed, where the final estimate is obtained from the extrapolation to $1/\langle d\rangle^2 \to 0$. The precise values that we used depended on the packing fraction, Reynolds number and composition, where we note that we studied 115 different combinations of these parameters. For dense systems ($\phi \approx 0.5$) with $\phi_1 = \phi_2$ and $d_1/d_2 = 2$ we typically evaluate α_i from the extrapolation of the data at $\langle d\rangle \approx 9$ and $\langle d\rangle \approx 18$.

Simulation Results for Monodisperse Systems

In Figure 3 we show our simulation data (symbols) for $\alpha(\phi, \mathrm{Re})$ multiplied by $(1-\phi)^2$, as a function of ϕ, together with the Ergun equation (dashed black line) and Eq. 7, from Hill, et al. (solid line). We find that for $\phi < 0.6$, our data is markedly different from the Ergun equation, and in reasonable agreement with the Hill, Koch and Ladd expression. It should be reminded, of course, that the Ergun equation is not expected to be valid for the entire packing fraction range, but only for dense systems. Our data clearly indicates that α is dependent on the Reynolds number, which implies that a linear scaling of the normalized drag force F with Re is an oversimplified representation in the range below Re = 1,000. This is shown more clearly in Figure 4, where we plot the same quantity $\alpha(1-\phi)^2$ but now as a function of the Reynolds number, for packing fraction $\phi = 0.6$ and $\phi = 0.2$. The lattice-Boltzmann data clearly indicate that α is not constant with respect to the Reynolds number, revealing a distinct peak at Re = 100 for $\phi = 0.4$. For $\phi = 0.5$ (not shown in the figure) we found a less pronounced peak at about the same position, whereas for lower-packing fractions the data seems to indicate that the peak has shifted to lower-Reynolds numbers, however, the range Re < 100 we have not resolved with sufficient detail in the simulations to determine the location of the maximum. Figure 4 also shows that the simulation data is in reasonable agreement with the correlation (7) by Hill et al., although the latter expression does not capture the dependence of α on the Reynolds number for $\phi = 0.6$, due to the fact that δF in Eq. 7, vanishes at this packing fraction. Note that this vanishing is not just an anomaly of our fit function (8), but does follow from the actual data of Hill et al.

Next, we test how well the "Wen and Yu"-type relations (4) can describe the simulation data. We recall that the Ergun type description was based on $F(\phi, 0)$, where we introduced a generalized function $\alpha(\phi, \mathrm{Re})$ to replace $1.75/18(1-\phi)^2$ in the Ergun equation. The Wen and Yu type description is based on $F(0, \mathrm{Re})$, where we now introduce a generalized function $\beta(\phi, \mathrm{Re})$ to replace the constant power 3.7 in the Wen and Yu equation. Before we evaluate β from the simulation data, however, we should first determine the best possible function $F(0, \mathrm{Re})$ for the drag on an isolated particle.

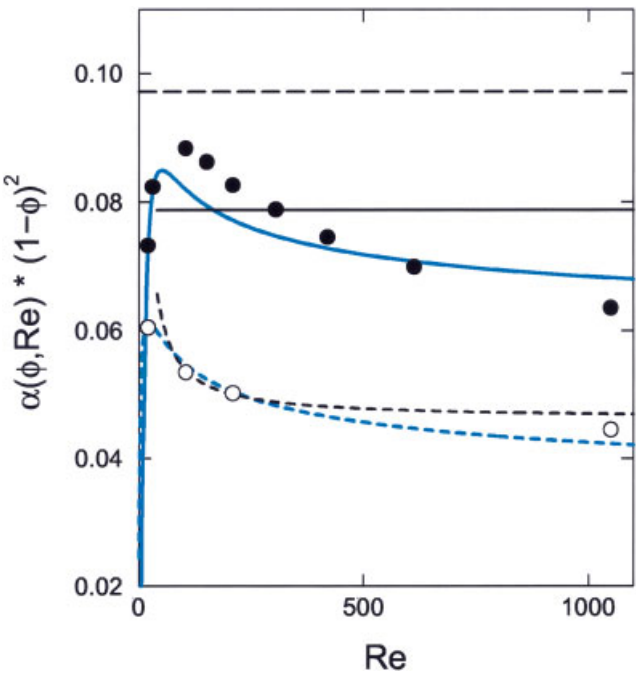

Figure 4. α multiplied by the porosity squared, as a function of the Reynolds number.

The filled circles, black solid line and grey solid line represent the simulation data, expression (7) by Hill et al.,[2] and expression (16) from this work, respectively, for $\phi = 0.6$. The open circles, black short-dashed line and grey short-dashed line represent the simulation data, expression (7), and expression (16), respectively, for $\phi = 0.2$. The long-dashed line represents the Ergun correlation $\alpha = 1.75/18$, which is independent of both ϕ and Re. [Color figure can be viewed in the online issue, which is available at www.interscience.wiley.com.]

To this end, we show in Figure 5 the simulation data for $F(\phi, \mathrm{Re})$ normalized by $F(\phi, 105)$, as a function of the Reynolds number. In this, the drag force F is calculated from the simulation data for α via $F(\phi, \mathrm{Re}) = F(\phi, 0) + \alpha\,\mathrm{Re}$, with $F(\phi, 0)$ given by Eq. 6. Note that the choice Re = 105 is quite arbitrary, but in this case most convenient since we have simulation data available at this Reynolds number for all packing fractions. If β is independent of the Reynolds number, then expression (4) gives that

$$\bar{F} = \frac{F(\phi, \mathrm{Re})}{F(\phi, 105)} = \frac{F(0, \mathrm{Re})}{F(0, 105)}$$

which is independent of the packing fraction. In Figure 5 it can be seen that the data for $\bar{F}$ for different ϕ do not fall onto a single curve, which indicates that it cannot be described by a function of the type (4), or more generally not by a product $f_1(\phi)f_2(\mathrm{Re})$, with f_1 and f_2 functions of the ϕ and Re only, respectively. If we would be forced to use such a description, however, then the function by White[37] for $F(0, \mathrm{Re})$ fits the data best, although the function by Dallavalle[38] (not shown in the figure) performs equally well. Note that this does not necessarily mean that the White correlation provides the best description for the drag on a single particle—it only seems the best choice for a Wen and Yu type drag correlation for Reynolds numbers higher than 100. We now cal-

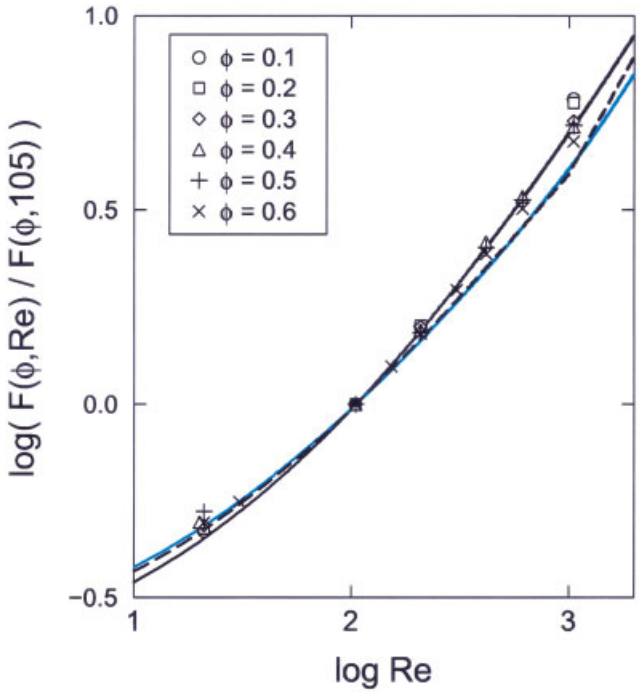

Figure 5. Log-log plot of the drag force *F* normalized to one at Re = 105 as a function of Re.

The symbols are the simulation data from this work for various packing fractions (see legend); the solid, dashed and grey lines are calculated from the correlations for $F(0, \mathrm{Re})$ by White, Schiller and Nauman, and Turton and Levenspiel, respectively (see Table 1). [Color figure can be viewed in the online issue, which is available at www.interscience.wiley.com.]

culate the exponent β from our simulation results for $F(\phi, \mathrm{Re})$ via

$$\beta(\phi, \mathrm{Re}) = -\log_{1-\phi}\left(\frac{F(\phi, \mathrm{Re})}{F(0, \mathrm{Re})}\right) \tag{15}$$

where the drag $F(0, \mathrm{Re})$ on a single particle is calculated from the correlation by White. Figure 6 shows that for $\phi \geq 0.3$ the power β is in the range of 3–4, but not constant as assumed in the Wen and Yu-equation. The value for β as calculated by Eq. 9 also varies between 3–4, but has the wrong trend when compared to the simulation data. Moreover, we find that β also clearly depends on ϕ. For the lowest packing fractions 0.2 and 0.1 the disagreement with the Wen and Yu exponent 3.7 is very large. Note that these results depend very much on the expression for $F(0, \mathrm{Re})$ that is used in Eq. 15. If the expression by Turton and Levenspiel[39] is used, then the data for $\phi = 0.5$ and 0.6 agrees reasonably well with Di Felice's expression 9, however, for $\phi = 0.1$ the power gets almost as high as 9.

From the comparison of our data with both the Ergun and Wen and Yu type expressions, the conclusion is that the former type is most suitable as a starting point when deriving a more refined drag force correlation. That is, it turns out to be more natural to describe the drag force in terms of a generalized $\alpha(\phi, \mathrm{Re})$, then in terms of a generalized power $\beta(\phi, \mathrm{Re})$. On the basis of our data, we suggest the following expression for α, which takes into account the dependence on both the packing fraction and the Reynolds number as shown in Figures 3 and 4

$$\alpha(\phi, \mathrm{Re}) = \frac{0.413}{24(1-\phi)^2} \times \left[\frac{(1-\phi)^{-1} + 3\phi(1-\phi) + 8.4\,\mathrm{Re}^{-0.343}}{1 + 10^{3\phi}\mathrm{Re}^{-(1+4\phi)/2}}\right] \tag{16}$$

The predictions for α calculated from this equation are given in Figures 3 and 4 by the grey lines. It can be seen that Eq. 16 does not provide a perfect fit, which is partly due to the scattering in the simulation data, and partly due to the fact that the drag force has a non trivial dependence on ϕ and Re, which cannot be captured by a single and relative simple function. Therefore, the function as suggested in Eq. 16 represents a compromise, where we put the emphasis on the accuracy at higher-Reynolds number, since for low Re the inertial contribution α Re to the total drag force F is relatively small. Combining the form drag (16) with the low-Reynolds number drag from reference I gives the final result for the normalized drag force at arbitrary Reynolds numbers and packing fractions

$$F(\phi, \mathrm{Re}) = \frac{10\phi}{(1-\phi)^2} + (1-\phi)^2\left(1 + 1.5\,\phi^{1/2}\right) + \frac{0.413\,\mathrm{Re}}{24(1-\phi)^2}\left[\frac{(1-\phi)^{-1} + 3\phi(1-\phi) + 8.4\,\mathrm{Re}^{-0.343}}{1 + 10^{3\phi}\mathrm{Re}^{-(1+4\phi)/2}}\right] \tag{17}$$

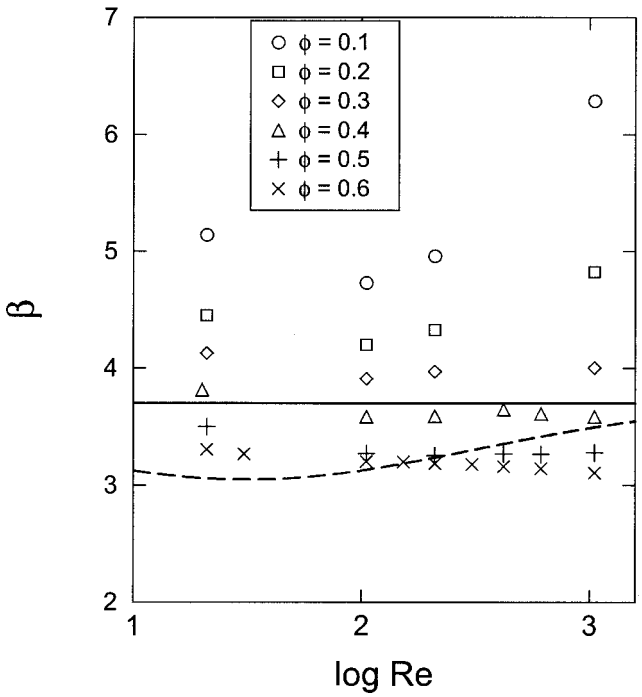

Figure 6. Exponent β in the Wen and Yu type drag relations (4), calculated from our simulation results for different packing fractions (points).

The solid line is the exponent 3.7 of the Wen and Yu equation,[11] the dashed line is expression (9) by Di Felice.[24]

Table 2. Relative Deviation ($F^{sim} - F$)/F^{sim} of the Total Drag force F^{sim} Obtained from the Lattice Boltzmann Simulations with the Various Correlations for F

Re ↓ ϕ →	0.100	0.200	0.300	0.400	0.450	0.500	0.550	0.600
21.0	−0.014	−0.019	0.008	0.002	–	−0.031	−0.024	−0.014
	−0.109	−0.123	−0.044	−0.013	–	−0.034	−0.020	−0.008
	0.167	0.178	0.072	0.065	–	0.041	0.054	0.072
30.5	–	–	–	–	–	–	–	−0.006
	–	–	–	–	–	–	–	0.020
	–	–	–	–	–	–	–	0.070
105.0	−0.054	−0.027	0.013	0.006	–	−0.054	–	0.039
	−0.099	−0.002	0.107	0.134	–	0.063	–	0.070
	0.167	0.174	−0.268	−0.185	–	−0.161	–	0.009
153.0	–	–	–	–	–	–	–	0.049
	–	–	–	–	–	–	–	0.063
	–	–	–	–	–	–	–	−0.034
210.0	−0.055	−0.014	0.030	0.015	–	−0.051	–	0.042
	−0.146	0.006	0.133	0.156	–	0.069	–	0.038
	0.221	0.235	−0.451	−0.340	–	−0.292	–	−0.089
420.0	–	–	–	0.029	–	−0.048	–	0.012
	–	–	–	0.155	–	0.049	–	−0.045
	–	–	–	−0.493	–	−0.428	–	−0.229
612.5	–	–	–	0.000	–	−0.065	–	−0.017
	–	–	–	0.115	–	0.015	–	−0.109
	–	–	–	−0.609	–	−0.514	–	−0.315
1049.4	0.027	0.038	−0.010	−0.033	−0.016	−0.074	−0.080	−0.074
	−0.243	−0.051	0.024	0.057	0.065	−0.025	−0.105	−0.218
	0.456	0.449	−0.932	−0.753	−0.648	−0.615	−0.534	−0.438

Top value: deviation with Eq. 17 proposed in this work. Middle value: deviation with the correlation (7) by Hill et al. Bottom value: deviation with the traditional correlations used in chemical engineering, which are the Wen and Yu[11] correlation for $\phi < 0.2$, and the Ergun[1] correlation for $\phi > 0.2$.

The relative deviation of the simulation data for F with Eq. 17, as well as with the correlation by Hill et al.,[2] and the combined Ergun and Wen and Yu correlation are shown in Table 2. It can be seen that the maximum deviation of the simulation data with Eq. 17 is 8%, where the average deviation is only 3%. Note that the functional form of Eq. 16 is chosen, such as to provide the best possible fit, and does not have any physical origin. However, the power 0.343 and the prefactor 0.413 are taken from the Turton and Levenspiel expression for $F(0, \mathrm{Re})$.[39] In the limit $\phi = 0$, Eq. 17 reduces to

$$F(0,\mathrm{Re}) = \frac{C_d\,\mathrm{Re}}{24} = 1 + \frac{0.145\,\mathrm{Re}^{0.657} + \frac{0.413}{24}\,\mathrm{Re}}{1 + \mathrm{Re}^{-1/2}}$$

which is compared with the other correlations from Table 1 in Figure 1.

Simulation Results for Bidisperse Systems

We have performed simulations for bidisperse systems at Reynolds numbers Re = 10, 100 and 500, packing fractions ϕ = 0.10, 0.25, 0.35, 0.40, 0.50, 0.60 and 0.65, dia. ratios d_2/d_1 = 4, 3, 2, 1.65 and 1.43, and mass ratios $\phi_2/\phi_1 \approx$ 20, 5, 3, 1, 1/3, and 1/9. We have not studied all combinations of these parameters, but limited ourselves to 120 different systems, with the emphasis on the higher-packing fractions and moderate-diameter ratios. In reference I it was found that for low Re, the individual drag force on the spheres could be well described by Eq. 13, that is, by the drag force of a monodisperse system multiplied by a correction term which depends on $y_i = d_i/\langle d\rangle$, and the packing fraction. Here we want to test if this correction is also valid for higher-Reynolds numbers. Thus, we assume that the following relation holds for the normalized individual drag force F_i on species i

$$F_i = ((1-\phi)\,y_i + \phi\,y_i^2 + 0.064(1-\phi)y_i^3)\,F(\phi,\langle\mathrm{Re}\rangle) \quad (18)$$

with $F(\phi, \langle\mathrm{Re}\rangle)$ the drag force for a monodisperse system at the same overall packing fraction, and Reynolds number equal to the average Reynolds number of the binary system, which is defined as

$$\langle\mathrm{Re}\rangle = \frac{\rho_g U\langle d\rangle}{\mu} \quad (19)$$

In Figure 7 we show $F_i/F(\phi, \langle\mathrm{Re}\rangle)$ as a function of the correction factor. The solid line represents Eq. 18, the symbols are the simulation data for F_i from all 120 systems that we studied, divided by $F(\phi, \langle\mathrm{Re}\rangle)$ as calculated from our best fit Eq. 17. On the basis of Figure 7 we can conclude that the correction factor which was derived for low Re, also applies to higher Re, which is to some extend remarkable since this correction factor was derived within the framework of the Darcy equation and the Carman-Kozeny approximation, which only hold for the limit of Stokes flow.

At present, in all chemical engineering models of gas-solid flows, no special modification is made for the drag force in bidisperse systems. That is, the drag force on an individual particle in such a system is simply assumed to be equal to the monodisperse drag force, with the dia. d replaced by the individual dia. d_i. In terms of the normalized drag forces as defined by Eq. 1 and 12, this corresponds to

$$F_i = F(\phi,\mathrm{Re}_i) \quad \text{with} \quad \mathrm{Re}_i = \frac{\rho_g U d_i}{\mu} = y_i\,\langle\mathrm{Re}\rangle \quad (20)$$

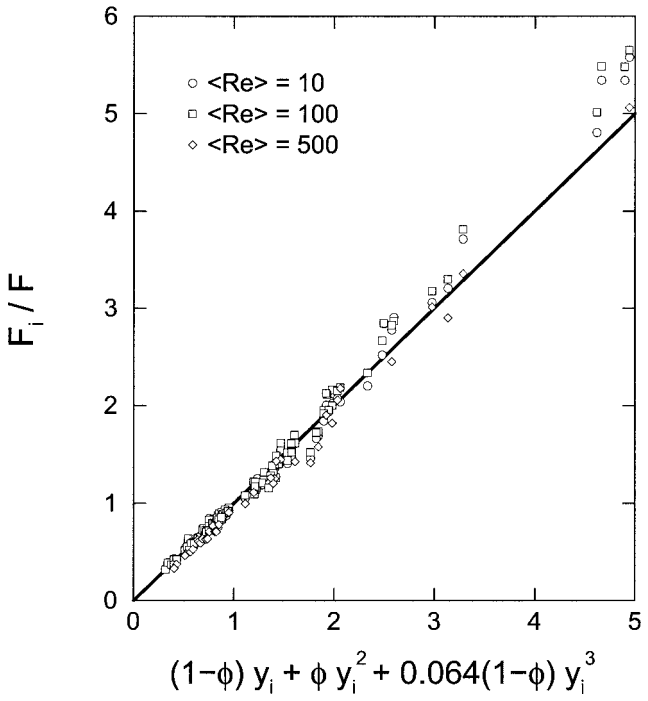

Figure 7. Ratio of the individual normalized drag force F_i of a bidisperse system to the monodisperse normalized drag force F.

The solid line represents Eq. 18, the points represent the simulation data for F_i, divided by F as calculated from (17), with Re the average-Reynolds number of the bidisperse system.

In Figures 8 to 10 we compare the LBM data for one particular packing fraction ($\phi = 0.5$) with expression Eq. 20. We find that for the small and large particles, the current drag models significantly over- respectively underpredict the individual drag force on the particles, and that the modification (Eq. 18) to F as proposed in this work provides a much better description of the individual drag force. In Figures 8–10 we also compare the LBM data to the theory by Patwardhan and Tien[32]. In their original theory, the average diameter in the calculation of δ (which is the average distance between a particle and its neighbours) is defined as $d_{\text{avg}} = x_1 d_1 + x_2 d_2$. However, this results in deviations of more than 100% with the LBM data, in particular for extreme diameter ratios and/or low porosities. A significant improvement can be made by using $d_{\text{avg}} = \langle d \rangle$ as defined by Eq. 11. The short-dashed line in Figures 8–10 is the result from the Patwardhan and Tien theory using $d_{\text{avg}} = \langle d \rangle$, and the average Reynolds number of the bidisperse systems. We find that there is now a very good agreement with the LBM simulation data. A similar trend was observed for the other packing fractions that we studied. On average the simulation data agrees within 10% with both expression Eq. 18, and the theory by Patwardhan and Tien. By contrast, the average deviation with Eq. 20 is 90%, with individual deviations that are as much as 350%. For packing fractions other than $\phi = 0.5$ a similar conclusion can be drawn.

Summary and Conclusions

In this work we have derived a new drag force relation for fluid flow past mono- and bidisperse arrays of spheres, on the basis of lattice-Boltzmann simulations. For monodisperse systems we suggest the following correlation for the normalized drag force

$$F(\phi, \mathrm{Re}) = \frac{10\phi}{(1-\phi)^2} + (1-\phi)^2\left(1 + 1.5\,\phi^{1/2}\right) + \frac{0.413\,\mathrm{Re}}{24(1-\phi)^2}\left[\frac{(1-\phi)^{-1} + 3\phi(1-\phi) + 8.4\,\mathrm{Re}^{-0.343}}{1 + 10^{3\phi}\mathrm{Re}^{-(1+4\phi)/2}}\right] \tag{21}$$

where ϕ is the solids volume fraction, and F and Re are defined by Eqs. 1 and 2. We found for monodisperse systems that the lattice-Boltzmann simulation data was consistent with previous lattice Boltzmann simulation results[2] (the average deviation being 8 %), however, our data for the form drag clearly exhibits a more complex functional form than the linear scaling with Re assumed by the Ergun-type correlation (Eq. 3). In particular, both in the monodisperse and the bidisperse simulations we found that α has a clear maximum around Re = 100 at high-packing fractions. Note that the data by Hill et al.[2] also indicate a deviation from linear scal-

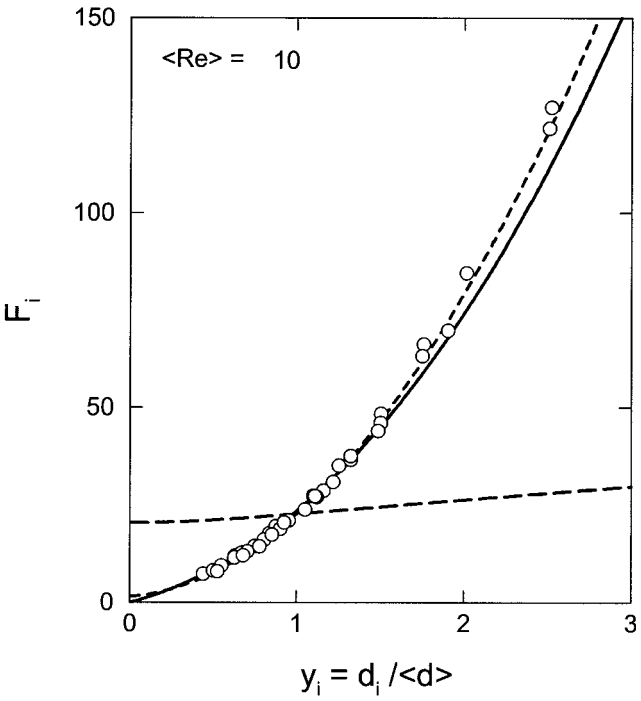

Figure 8. Individual normalized drag force F_i of a bidisperse system as a function of the diameter over the average diameter, for Re = 10.

The points are the simulation data, the lines are the various predictions based on expression (17) for the monodisperse drag force. The solid line is calculated from equation (18), the short dashed line the prediction from the theory by Patwardhan and Tien,[32] and the long-dashed line is calculated from Eq. 20. Note that the latter is used in almost all numerical models for large-scale gas-solid flows. The packing fraction for this system is equal to 0.5.

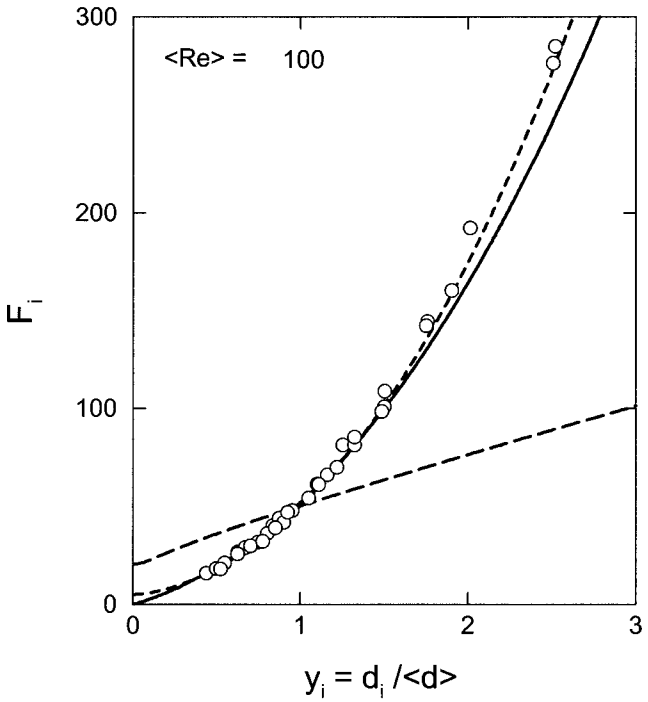

Figure 9. As Figure 8, but now for Re = 100.

ing, however, this has not been included explicitely in their correlation; the deviation shown in Figure 4 for $\phi = 0.2$ is due to the extra term δF/Re in Eq. 7, which we constructed on the basis of the Hill-Koch-Ladd data. In our new correlation (Eq. 21), the deviations from linear scaling have been taken into account, leading to an average deviation of 3 % with the simulation data. By contrast, our data deviates substantially (more than 100%) from the Ergun correlation, where we found that the latter equation under- respectively over-predicts the drag force at low- and high-Reynolds numbers. The same conclusion was drawn by Hill et al.[2] If we rule out any errors in the determination of $\bigtriangledown P$, μ, and ϕ in the experiments by Ergun, then the only cause of the deviation of his data with the lattice-Boltzmann results could lie in the fact that the particulate systems in the experiments are not as well-defined—in terms of homogeneity and monodispersity—as in the simulations. In some of the experiments, the beds consist of crushed coke particles, with volume fractions in the range 0.46–0.56. In reference I it was argued that for low-Reynolds numbers, a size distribution could decrease the pressure drop substantially, when compared to a perfect monodisperse system. Also the fact that the coke particles in the experiment are nonspherical could have an influence. The diameter D that appears in Ergun's equation is that of a sphere, which has the same surface area as the coke particles, which would cancel the effect of the irregular shape, at least in the Carman-Kozeny approximation, that is, for low-Reynolds numbers. However, Ergun also mentions that the particles are oriented by the gas flow, which would decrease the pressure drop. Another argument for the difference with Ergun is given by Hill et al.[2] They argued that the rather loose packing fraction of 0.46–0.56 would require a network of touching particles. Compared to a random array of nontouching particles, such a network would increase the drag force at higher-Reynolds numbers, whereas it would decrease the drag force at low-Reynolds numbers.

We should note that in the simulations at the highest packing fraction ($\phi = 0.60$) the systems showed some ordering, where in snapshots the underlying structure of a BCC-type lattice could be identified. Also the $\phi = 0.55$ configurations revealed some very weak structure, although much less then for $\phi = 0.60$. In previous simulation studies,[2] it was shown that for ordered systems at larger Reynolds numbers, the drag force very much depends on the flow direction; that is, a large difference was found between flow along one of the main lattice directions, and a random direction. Therefore, for our final estimate for the drag force we averaged the results from 2–3 different random-flow directions, where we found that the variation in F for these directions was on the same level as the variation from the different configurations. In this respect we would also like to point out that in practical situations (for examples, dense gas-fluidized beds) at high-packing fractions, some ordering will be inevitable, so that the systems we studied can be considered representative for dense beds of particles. For systems with packing fractions of 0.50, and lower, there was no evidence of order in the configuration.

For bidisperse systems, we found that the individual drag force on a particle of species i can be well represented by

$$F_i = ((1-\phi)\,y_i + \phi\,y_i^2 + 0.064(1-\phi)y_i^3)\,F(\phi, \langle \mathrm{Re} \rangle), \qquad y_i = \frac{d_i}{\langle d \rangle} \tag{22}$$

with F_i, $\langle d \rangle$ and $\langle \mathrm{Re} \rangle$ defined by Eq. 12, Eq. 11, and Eq. 19 and where F is given by the monodisperse expression (Eq. 21).

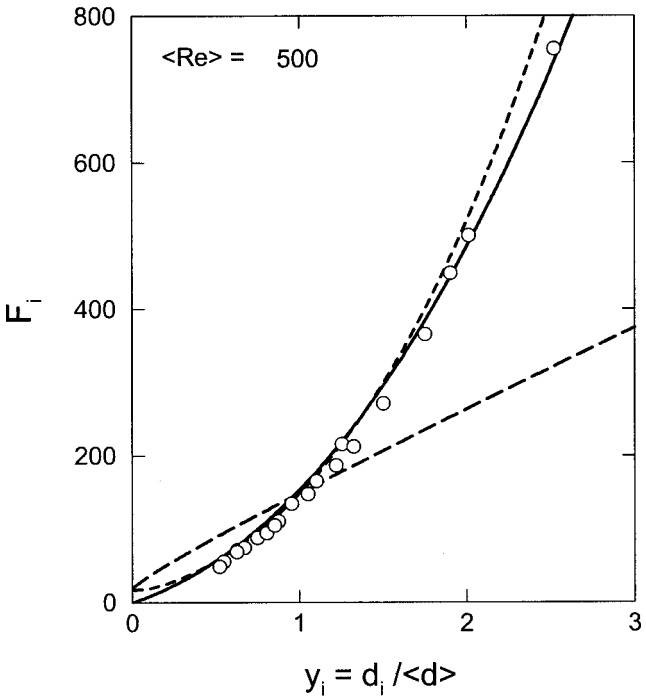

Figure 10. As Figure 8, but now for Re = 500.

For the largest diameter ratios that we studied, we found that the deviation can be as much as a factor of 3 with estimates for F_i, that are currently used in the larger scale models gas-solid flow. In particular for flow-driven segregation phenomena, we expect that the modification to F given in Eq. 22 will have a large impact on the results. Simulation studies of segregation in a laboratory scale bidisperse-fluidized beds, using a hybrid discrete-particle model—computational fluid dynamics model, are reported elsewhere.[40] Finally, we expect that the relation (Eq. 22) is also valid for general polydisperse systems. Some preliminary simulation data for a 4 species system with diameter ratios 1:2:3:4 were in very good agreement with expression (Eq. 22), however, much more extensive simulations are required to come to any definite conclusions. It should also be stressed that the drag relation that we propose is for *static* arrays of spheres, whereas in many practical applications the particles are moving about. The precise effect of the granular temperature on the drag force is very much an open issue, and is one of the important topics which still needs to be addressed in this field of research.

Acknowledgments

For the simulation we have used the lattice Boltzmann suspension code SUSP3D developed by Anthony Ladd. We thank him for allowing us to use his code. This work is part of the research program of the "Stichting voor Fundamenteel Onderzoek der Materie (FOM)", which is financially supported by the "Nederlandse Organisatie voor Wetenschappelijk Onderzoek (NWO)". This work is also sponsored by the National Computing Facilities Foundation (NCF) for the use of supercomputer facilities, with financial support from NWO.

Literature Cited

1. Ergun S. Fluid flow through packed columns. *Chem Eng Proc*. 1952;48:89.
2. Hill RJ, Koch DL, Ladd AJC. Moderate-Reynolds-number flows in ordered and random arrays of spheres. *J Fluid Mech*. 2001;448:243.
3. Kim S, Russel WB. Modeling of porous media by renormalization of the Stokes equation. *J Fluid Mech*. 1985;154:269.
4. Happel J, Brenner H. Low Reynolds Number Hydrodynamics. Dordrecht: Martinus Nijhoff; 1986.
5. Goldstein S. Concerning some solutions of the boundary layer equations in hydrodynamics. *Proc Cambridge Philos Soc*. 1929;26:1.
6. Clift R, Grace JR, Weber ME. Bubbles, Drops and Particles. New York: Academic Press; 1978.
7. Kaneda Y. The drag on a sparse random array of fixed spheres in flow at small but finite Reynolds number. *J Fluid Mech.* 1986;167:455.
8. Koch DL, Ladd AJC. Moderate Reynolds number flows through periodic and random arrays of aligned cylinders. *J Fluid Mech.* 1997;349: 31.
9. Hill RJ, Koch DL, Ladd AJC. The first effects of fluid inertia on flow in ordered and random arrays of spheres. *J Fluid Mech.* 2001;448: 213.
10. Di Felice R. Hydrodynamics of liquid fluidisation. *Chem Eng Sci*. 1995;50:1213.
11. Wen CY, Yu YH. Mechanics of fluidization. *AIChE J*. 1966;62:100.
12. Van der Hoef MA, Beetstra R, Kuipers JAM. Lattice Boltzmann simulations of low Reynolds number flow past mono- and bidisperse arrays of spheres: results for the permeability and drag force. *J Fluid Mech*. 2005;528:233.
13. Van der Hoef MA, van Sint Annaland M, Kuipers JAM. Computational fluid dynamics for dense gas-solid fluidized beds: a multiscale modeling strategy. *Chem Eng Sci*. 2004;59:5157.
14. Blake, FE. *Trans Am Inst Chem Engrs*. 1922;14:415.
15. Kozeny J. *Akad Wiss Wien Math.-naturw, Klasse*. 1927;136:271.
16. Burke SP, Plummer WB. Gas flow through packed columns. *Ind Eng Chem.* 1928;20:1196.
17. Fand RM, Kim BYK, Lam ACC, Phan RT. Resistance to the flow of fluids through simple and complex porous media whose matrices are composed of randomly packed spheres. *Trans ASME: J Fluids Eng*. 1987;109:268.
18. Maier RS, Kroll DM, Davis HT, Bernard RS. Simulation of flow in bidisperse spheres packings. *J Colloid Interface Sci*. 1999;217: 341.
19. Carman, PC. Fluid flow through granular beds. *Trans Inst Chem Eng*. 1937;15:150.
20. Kandhai D, Derksen JJ, van den Akker HEA. Interphase drag coefficients in gas-solid flows. *AIChE J*. 2003;49:1060.
21. Schlichting H. Boundary-Layer Theory. New York: McGraw-Hill Book Company; 1979.
22. Richardson JF, Zaki WN. *Sedimentation and fluidisation*. Part I. *Trans Instn Chem Engrs*. 1954;39:175.
23. Schiller L, Nauman A. A drag coefficient correlation. *VDI Zeitung*. 1935;77:318.
24. Di Felice R. On the voidage function in two-phase multiparticle systems. *Int J Multiphase Flow*. 1994;20:153.
25. Gidaspow D. Multiphase flow and fluidization: Continuum and kinetic theory descriptions. Boston: Academic Press; 1994.
26. Gibilaro LG, Di Felice R, Waldram SP, Foscolo PU. Generalized friction factor and drag coefficient correlations for fluid-particle interactions. *Chem Eng Sci*. 1985;40:1817.
27. Batchelor GK. Sedimentation in a dilute polydisperse system of interacting spheres. Part 1. General theory. *J Fluid Mech*. 1982;119: 379.
28. Batchelor GK, Wen CS. Sedimentation in a dilute polydisperse system of interacting spheres. Part 2. Numerical results. *J Fluid Mech*. 1982;124:495.
29. Liang SC, Hong T, Fan LS. Effects of particle arrangements on the drag force of a particle in the intermediate flow regime. *Int J Multiphase Flow*. 1996;22:285.
30. Katoshevski D, Zhao B, Ziskind G, Bar-Ziv E. Experimental study of the drag force acting on a heated particle. *J Aerosol Sci*. 2001; 32:73.
31. Zhu C, Lam K, Chu HH, Tang XD, Lui G. Drag forces of interacting spheres in power-law fluids. *Mech Res Comm*. 2003;30:651.
32. Patwardhan VS, Tien C. Sedimentation and liquid fluidization of solid particles of different sizes and density. *Chem Eng Sci*. 1985; 40:1051.
33. Okayama Y, Doi A, Kawaguchi T, Tanaka T, Tsuji Y. Drag force model for fluidized bed of binary mixture of particles. *Proceedings of the 5th World Congress on Particle Technology (WCPT5),* Orlando, FL; April 23–27; 2006.
34. Succi S. The lattice Boltzmann equation for fluid dynamics and beyond. Oxford: Clarendon Press; 2001.
35. Ladd, AJC. Numerical simulations of particulate suspensions via a discretized Boltzmann equation (Part I + II). *J Fluid Mech.* 1994; 271:285.
36. Hasimoto H. On the periodic fundamental solutions of the Stokes equation and their application to viscous flow past a cubic array of spheres. *J Fluid Mech*. 1959;5:317.
37. White FM. Viscous fluid flow. pp 206–210. New York: McGraw-Hill; 1974.
38. Dallavalle JM. Micromeretics: the technology of fine particles. London: Pitman; 1948.
39. Turton R, Levenspiel O. A short note on the drag correlation for spheres. *Powder Tech*. 1986;47:83.
40. Beetstra R, van der Hoef MA, Kuipers JAM. Numerical study of segregation using a new drag force correlation for polydisperse systems derived from lattice Boltzman simulations. *Chem Eng Sci*. 2007;62:246.

Manuscript received Mar. 8, 2006, and revision received Sept. 9, 2006, and final revision received Nov. 2, 2006.